Local sliding mode inversion algorithms and state observers with space applications

Received: Added at production | Revised: Added at production | Accepted: Added at production

DOI: xxx/xxxx

RESEARCH ARTICLE

Local sliding mode inversion algorithms and state observers with space applications

Corrado Possieri*[1,2] | Carlo Novara[3]

[1]Dipartimento di Ingegneria Civile e Ingegneria Informatica, Università di Roma Tor Vergata, 00133 Roma, Italy
[2]Istituto di Analisi dei Sistemi ed Informatica "A. Ruberti", Consiglio Nazionale delle Ricerche, 00185 Roma, Italy
[3]Dipartimento di Elettronica e Telecomunicazioni, Politecnico di Torino, 10129 Torino, Italy

Correspondence
*Corrado Possieri. Email: corrado.possieri@uniroma2.it

Present Address
Via del Politecnico, 1, 00133 Roma, Italy

Summary

The main objective of this work is to propose novel finite-time algorithms to either invert a time-varying map or to estimate the state of a time-varying nonlinear plant. The former goal is pursued by using a sliding mode version of the Newton algorithm, whereas the latter objective is achieved by resorting to the inverse of the Jacobian matrix of the observability map to implement a sliding mode differentiator in the original coordinates. Finally, it is shown how these two techniques can be efficiently used to solve some relevant space applications, such as the estimation of the angular velocity of an axial symmetric satellite, the estimation of the inertia parameters of an orbiting object from measurements of its angular velocities, and the estimation of a Keplerian orbital element given measurements of the other five ones.

KEYWORDS:
Nonlinear models and systems, sliding mode control, identification, control applications

1 | INTRODUCTION

The problem of estimating the state of a system is of paramount importance in several practical applications either to design a controller or to gather information about the current working conditions of the observed plant [1]. When dealing with linear plants, the problem of estimating its state can be dealt with using well-established tools such as the Luenberger observer [2] and the Kalman filter [3]. On the other hand, the problem of designing state observers for nonlinear systems is significantly more challenging. Several design methods have been proposed in the technical literature to deal with this problem, such as the extended Kalman filter (EKF) [4], particle filters [5], Lyapunov based observers [6], Luenberger-like approaches [7], linearization via output injection [8], and high-gain observers [9]. One of the mostly employed techniques to design state observers for nonlinear plants consists in determining a change of coordinates that allows to rewrite the dynamics of the system as a chain of integrators (usually referred to as *canonical observability form* [10]), estimating the state of the system in these transformed coordinates using a system capable of estimating the time derivatives of the measured output (such as sliding mode differentiators [11], high-gain observers [12], or super twisting algorithms [13]), and using an inverse of the change of coordinates to estimate the current state of the system in the original coordinates.

If a closed-form for the inverse change of coordinates is not available, a possible approach to tackle the observer design problem is to resort to dynamical inversion algorithms [14,15,9]. Several techniques have been proposed in the literature to invert time-invariant maps, such as Newton [15,16], gradient [17], and sliding mode [18] algorithms. However, in the case that the system to be observed is time-varying, the change of coordinates that transforms the system in canonical observability form is time-varying as well, and hence the above mentioned techniques cannot be directly used to design a state observer for the system.

The main goal of this work is twofold. On one hand, a sliding mode inversion algorithm is proposed to invert time-varying maps without any knowledge about the dynamics of the input signal. On the other hand, an alternative observer design technique

is proposed, which, working directly in the original coordinates, allows one to design a local state observer, whose state converges in finite-time to the state of the observed plant. The sliding mode inversion algorithm uses a modified version of the Newton algorithm [18,16] to dynamically determine, in finite-time, the signal that is generating the measured output. The observer design strategy is similar to the one employed in the literature [19] to design Luenberger-like observers for nonlinear systems: the dynamics of an observer working for a system in canonical observability form are implemented in the original coordinates by resorting to the inverse of the Jacobian of the observability map. However, while in the literature the design usually relies on high-gain observers [20], hence guaranteeing just asymptotic convergence of the estimation error to zero, in this paper it relies on sliding mode differentiators [21], thus ensuring finite-time convergence of the estimation error to zero. It is worth pointing out that finite-time convergence of the estimation error to zero can be achieved also using other methods available in the literature [22,23]. However, global homogeneous in the bi-limit observers [22] require that the system is already in observability canonical form, whereas the observer proposed in this work can be implemented directly in the original coordinates. Further, differently from other observers available in the literature [23], the one proposed in this paper does not require that the system is linearizable by output injection.

Finally, the proposed observer design methods are applied to solve space applications such as the estimation of the angular velocity of an axial symmetric satellite, the estimation of the inertia parameters of an orbiting object from measurements of its angular velocities, and the estimation of a Keplerian orbital element given measurements of the other five ones.

2 | SLIDING MODE INVERSION OF TIME-VARYING MAPS

Given a time-varying map $h(t,x)$, $h : \mathbb{R}_{\geq 0} \times \mathbb{R}^n \to \mathbb{R}^n$, and a $\mathcal{C}^1$ signal $x(t) \in \mathcal{X}$, $\mathcal{X} \subset \mathbb{R}^n$, consider the output signal

$$y(t) = h(t, x(t)).$$

The main objective of this section is to design a sliding mode algorithm that, on the basis of measurements of the signal $y(t)$ and the knowledge of the function $h(t,x)$, is capable of reconstructing the signal $x(t)$. Toward this goal, for any $\varepsilon \in \mathbb{R}_{>0}$, define the open ball $\mathcal{B}_\varepsilon$ of radius ε, $\mathcal{B}_\varepsilon = \{x \in \mathbb{R}^n : \|x\|_2 < \varepsilon\}$, and the set $\mathcal{X}_\varepsilon = \{x \in \mathbb{R}^n : x - \hat{x} \in \mathcal{X}, \forall \hat{x} \in \mathcal{B}_\varepsilon\}$. The following three assumptions are made all throughout this section.

Assumption 1. The set $\mathcal{X}$ is bounded and there exists $\varepsilon > 0$ such that $x(t) \in \mathcal{X}_\varepsilon$ for all $t \geq 0$.

Assumption 2. The function $x \mapsto h(t,x)$ is $\mathcal{C}^1$ and bijective over $\mathcal{X}$ for all $t \geq 0$, its inverse $y \mapsto h^{-1}(t,y)$ is $\mathcal{C}^1$ for all $t \geq 0$, and there exist constants $\varsigma_1, \varsigma_2 \in \mathbb{R}_{>0}$ such that, for all $x, \hat{x} \in \mathcal{X}$ and all $t \geq 0$,

$$\varsigma_1 \|h(t,x) - h(t,\hat{x})\|_2 \leq \|x - \hat{x}\|_2 \leq \varsigma_2 \|h(t,x) - h(t,\hat{x})\|_2. \tag{1}$$

Note that if both h and its inverse h^{-1} are locally Lipschitz in $\mathcal{X}$, then the bounds in (1) are satisfied.

Assumption 3. The signal $\dot{y}(t)$ is bounded.

By noticing that $\dot{y}(t) = \frac{\partial h(t,x(t))}{\partial t} + \frac{\partial h(t,x(t))}{\partial x}\dot{x}(t)$, Assumption 3 is satisfied if $(t,x) \mapsto \|\frac{\partial h(t,x(t))}{\partial t}\|$ and $(t,x) \mapsto \|\frac{\partial h(t,x(t))}{\partial x}\|$ are both bounded for all $(t,x) \in \mathcal{X}_\varepsilon$ and $\|\dot{x}(t)\|$ is bounded, provided that Assumption 1 holds.

Thus, define the Jacobian matrix

$$J(t,x) = \frac{\partial h(t,x)}{\partial x},$$

which, under Assumptions 1 and 2, has full rank for all $x \in \mathcal{X}$ and all $t \geq 0$ (see [24] Section 1.2). Thus, consider the following sliding mode inversion algorithm

$$\dot{\hat{x}}(t) = \mu\, J^{-1}(t,\hat{x}(t)) \left(\operatorname{sign}(y(t) - h(t,\hat{x}(t))) - \frac{\partial h(t,\hat{x}(t))}{\partial t}\right), \tag{2}$$

where $\mu \in \mathbb{R}_{>0}$ is a tuning constant and $\operatorname{sign}(\cdot)$ denotes the entry-wise sign function (see [21] Equations (1.13) and (1.14)),

$$\operatorname{sign}(\sigma_i) = \begin{cases} 1, & \text{if } \sigma_i > 0, \\ [-1,1], & \text{if } \sigma_i = 0, \\ -1, & \text{if } \sigma_i < 0, \end{cases} \qquad i = 1, \dots, n.$$

Since the right-hand side of system (2) is discontinuous, its solutions have to be understood in the Filippov sense (see[25] §4, Chapter 4). The following theorem shows that, under Assumptions 1, 2, and 3, the sliding mode inversion algorithm (2) is capable of reconstructing locally and in finite-time the signal $x(t)$.

Theorem 1
Let Assumptions 1, 2, and 3 hold, and let $\tilde{x}(t) = x(t) - \hat{x}(t)$. There exist $\mu^\star \in \mathbb{R}_{>0}$ and $\delta^\star \in \mathbb{R}_{>0}$ such that if $\|\tilde{x}(0)\|_2 \leq \delta^\star$ and $\mu \geq \mu^\star$, then there exists a finite time $\Upsilon \in \mathbb{R}_{\geq 0}$ such that $\hat{x}(t) = x(t)$ for all $t \geq \Upsilon$.

Proof. Let $\hat{y}(t) = h(t, \hat{x}(t))$, and, using the convention $\inf_{t\in\emptyset} t = +\infty$, let

$$T := \inf\{t \in \mathbb{R}_{\geq 0} : \tilde{x}(t) \notin \mathcal{B}_\varepsilon\}.$$

In particular, if there exist times $\tau \in \mathbb{R}_{\geq 0}$ such that $\tilde{x}(\tau) \notin \mathcal{B}_\varepsilon$, then T is the infimum of such times, otherwise it equals $+\infty$. Hence, since $\hat{x}(t) = x(t) - \tilde{x}(t)$ and $x(t) \in \mathcal{X}_\varepsilon$, under Assumption 1, one has that $\hat{x}(t) \in \mathcal{X}$ for all $t \in [0, T)$ and there is no finite escape time for all $t \in [0, T)$ even in the case that $T = +\infty$. Thus, letting $\tilde{y}(t) = y(t) - \hat{y}(t)$, consider the Lyapunov function $V(t) = \|\tilde{y}(t)\|_2^2$. For all $t \in [0, T)$, the time-derivative of $V(t)$ satisfies

$$\begin{aligned}\dot{V}(t) &= \tilde{y}^\top(t)\left(\dot{y}(t) - J(t, \hat{x}(t))\dot{\hat{x}}(t) + \frac{\partial h(t, \hat{x}(t))}{\partial t}\right)\\ &= \tilde{y}^\top(t)\dot{y}(t) - \mu\,\|\tilde{y}(t)\|_1\\ &\leq -\left(\mu - \|\dot{y}(t)\|_2\right)\sqrt{V(t)}.\end{aligned}$$

This implies that[26], for all $t \in [0, T)$, one has that

$$V(t) \leq \max\left\{\frac{1}{4}\left(2\|\tilde{y}(0)\|_2 + \int_0^t \|\dot{y}(\tau)\|_2 \mathrm{d}\tau - \mu\, t\right)^2, 0\right\},$$

i.e., by the definition of V and (1), for all $t \in [0, T)$, one has that

$$\|\tilde{y}(t)\|_2 \leq \max\left\{\|\tilde{y}(0)\|_2 + \frac{1}{2}\int_0^t \|\dot{y}(\tau)\|_2 \mathrm{d}\tau - \frac{1}{2}\,\mu\, t, 0\right\}, \tag{3a}$$

$$\|\tilde{x}(t)\|_2 \leq \max\left\{\varsigma_2\,\|\tilde{y}(0)\|_2 + \frac{\varsigma_2}{2}\int_0^t \|\dot{y}(\tau)\|_2 \mathrm{d}\tau - \frac{\varsigma_2}{2}\,\mu\, t, 0\right\} \leq \max\left\{\frac{\varsigma_2}{\varsigma_1}\,\|\tilde{x}(0)\|_2 + \frac{\varsigma_2}{2}\int_0^t \|\dot{y}(\tau)\|_2 \mathrm{d}\tau - \frac{\varsigma_2}{2}\,\mu\, t, 0\right\}. \tag{3b}$$

Therefore, under Assumption 3, there exist $\mu^\star \in \mathbb{R}_{>0}$ and $\delta^\star \in \mathbb{R}_{>0}$ such that, if $\|\tilde{x}(0)\|_2 \leq \delta^\star$ and $\mu \geq \mu^\star$, then $T = +\infty$, i.e., there does not exist a time $t \in \mathbb{R}_{\geq 0}$ such that $\tilde{x}(t) \notin \mathcal{B}_\varepsilon$, and $\tilde{x}(t)$ converges in finite-time to 0. □

Remark 1. The proof of Theorem 1 allows one to estimate the settling time of the proposed finite-time inversion algorithm. Namely, if $\|\tilde{x}(0)\|_2 \leq \delta^\star$ and $\|\dot{y}(t)\|_2 \leq Y$ for all $t \geq 0$, one has that $\Upsilon \leq \frac{2\delta^\star}{\varsigma_1(\mu - Y)}$. This further shows that the settling time of the sliding mode inversion algorithm (2) can be made arbitrarily small by increasing the design parameter μ.

The following remark shows that the dynamics of the sliding mode inversion algorithm (2) can be simplified in the case that $\frac{\partial h(t,x)}{\partial x}$ is bounded for all $(t, x) \in \mathbb{R}_{\geq 0} \times \mathbb{R}^n$.

Remark 2. In view of the proof of Theorem 1, if $\frac{\partial h(t,x)}{\partial x}$ is bounded for all $(t, x) \in \mathbb{R}_{\geq 0} \times \mathbb{R}^n$, then the dynamics of the sliding mode inversion algorithm (2) can be simplified as

$$\dot{\hat{x}}(t) = \mu\, J^{-1}(t, \hat{x}(t))\,\mathrm{sign}(y(t) - h(t, \hat{x}(t))). \tag{4}$$

In fact, in such a case, the time-derivative of the Lyapunov function V defined in the proof of Theorem 1 satisfies

$$\dot{V}(t) \leq -\left(\mu - \|\dot{y}(t)\|_2 - \left\|\frac{\partial h(t, \hat{x})}{\partial t}\right\|_2\right)\sqrt{V(t)},$$

for all $t \in [0, T)$. Therefore, following the same reasoning given in the proof of Theorem 1, if in addition to the hypotheses of such a theorem one has also that $\frac{\partial h(t,x)}{\partial x}$ is bounded for all $(t, x) \in \mathbb{R}_{\geq 0} \times \mathbb{R}^n$, then the sliding mode inversion algorithm (4)

converges in finite-time to the signal $x(t)$. Note that this is particularly useful when the values attained by $\frac{\partial h(t,x)}{\partial x}$ cannot be directly measured such as when they are generated by an external process.

By Theorem 1, the solution $\hat{x}(t)$ to the sliding mode inversion algorithm (2) locally converges in finite-time to the signal $x(t)$. The following corollary shows that the convergence is in fact global in the case that Assumption 2 is strengthened.

Corollary 1
Let Assumption 2 hold with $\mathcal{X} = \mathbb{R}^n$ and let Assumption 3 hold. There exists $\mu^\star \in \mathbb{R}_{>0}$ such that, if $\mu \geq \mu^\star$, then the solution $\hat{x}(t)$ of system (2) converges in finite-time to $x(t)$.

Proof. If Assumption 2 holds with $\mathcal{X} = \mathbb{R}^n$, then $J(t,x)$ has full rank for all $x \in \mathbb{R}^n$ and all $t \geq 0$. Thus, using the same construction employed in the proof of Theorem 1, there exists $\mu^\star \in \mathbb{R}_{>0}$ such that if $\mu \geq \mu^\star$, then $T = +\infty$ and the estimation error $\tilde{x}(t)$ converges in finite-time to 0. □

It is worth noticing that although Corollary 1 guarantees that $\hat{x}(t)$ converges in finite-time to $x(t)$, by (3b), the convergence time depends on the norm of the initial error $\tilde{x}(0)$. In particular, larger initial errors lead to larger convergence time of the sliding mode algorithm (2).

The main goal of the remainder of this section is to characterize the robustness of the sliding mode inversion scheme (2) with respect to measurement noise. Hence, consider the following theorem.

Theorem 2
Let Assumptions 1, 2, and 3 hold, and let $\tilde{x}(t) = x(t) - \hat{x}(t)$.

Suppose that an additive noise $d(t)$ is added to the signal $y(t)$ and that $\|\dot{d}(t)\|_2$ is bounded. There exist $\mu^\star \in \mathbb{R}_{>0}$, $\delta^\star \in \mathbb{R}_{>0}$, and $\Delta^\star \in \mathbb{R}_{>0}$ such that, if $\|\tilde{x}(0)\|_2 \leq \delta^\star$, $\mu \geq \mu^\star$, and $\|d(t)\|_2 \leq \Delta^\star$, then there exists a finite time $\Upsilon \in \mathbb{R}_{\geq 0}$ such that $\|\hat{x}(t) - x(t)\| \leq \varsigma_2 \Delta^\star$ for all $t \geq \Upsilon$.

Proof. Let T be defined as in the proof of Theorem 1. Using the same reasoning employed in such a proof, letting $\check{y}(t) = y(t) + d(t)$ and $\check{y}(t) = \check{y}(t) - \hat{y}(t)$, one has that, for all $t \in [0, T)$,

$$\|\check{y}(t)\|_2 \leq \max\left\{ \|\check{y}(0)\|_2 + \frac{1}{2}\int_0^t \|\dot{y}(\tau) + \dot{d}(\tau)\|_2 \mathrm{d}\tau - \frac{1}{2}\mu\, t, 0 \right\},$$

$$\|\tilde{x}(t)\|_2 \leq \varsigma_2 \|d(t)\|_2 + \max\left\{ \varsigma_2 \|d(0)\| + \frac{\varsigma_2}{\varsigma_1}\|\tilde{x}(0)\|_2 + \frac{\varsigma_2}{2}\int_0^t \|\dot{y}(\tau) + \dot{d}(\tau)\|_2 \mathrm{d}\tau - \frac{\varsigma_2}{2}\mu\, t, 0 \right\}.$$

Thus, the proof of the theorem follows from the same reasoning used to prove Theorem 1. □

3 | SLIDING MODE STATE OBSERVER FOR TIME-VARYING DYNAMICAL SYSTEMS

In Section 2, a sliding mode dynamical algorithm has been proposed to dynamically invert time-varying maps. The main objective of this section is to show how similar techniques can be applied to estimate the state of time-varying dynamical systems. Namely, consider the time varying system

$$\dot{x}(t) = f(t, x(t)), \tag{5a}$$

$$y(t) = h(t, x(t)), \tag{5b}$$

where $x(t) \in \mathbb{R}^n$ is the state of the system, $f : \mathbb{R}_{\geq 0} \times \mathbb{R}^n \to \mathbb{R}^n$ is a smooth map, $y(t) \in \mathbb{R}$ is the output of the plant, and $h : \mathbb{R}_{\geq 0} \times \mathbb{R}^n \to \mathbb{R}$ is a smooth map. Thus, define the functions

$$D_f^0 h(t,x) = h(t,x),$$

$$D_f^{i+1} h(t,x) = \frac{\partial D_f^i h(t,x)}{\partial x} f(t,x) + \frac{\partial D_f^i h(t,x)}{\partial t}, \quad i = 1, \dots, n-2.$$

The main role of these functions is to relate the current state of system (5) with the time derivatives of the output $y(t)$. In particular, it can be easily derived that, for all times $t \geq 0$, one has that

$$\frac{\mathrm{d}^i y(t)}{\mathrm{d}t^i} = D_f^i h(t, x(t)), \quad i = 0, \dots, n-1. \tag{6}$$

Thus, define the observability map of system (5),

$$O(t,x) = \begin{bmatrix} D_f^0 h(t,x) \\ D_f^1 h(t,x) \\ \vdots \\ D_f^{n-1} h(t,x) \end{bmatrix}.$$

By (6), letting $z(t) = [\, z_1(t) \ \cdots \ z_n(t) \,]^\top$,

$$z(t) = \begin{bmatrix} y(t) \\ \frac{\mathrm{d}y(t)}{\mathrm{d}t} \\ \vdots \\ \frac{\mathrm{d}^{n-1}y(t)}{\mathrm{d}t^{n-1}} \end{bmatrix},$$

one has that $z(t) = O(t, x(t))$ for all $t \geq 0$.

In view of Theorem 1, if the following three assumptions hold

- the state $x(t)$ of system (5) lies in the compact set $\mathcal{X}_\varepsilon$,
- the observability map $O(t,x)$ satisfies Assumption 2,
- the time-derivative $\dot{z}(t)$ of $z(t)$ is bounded,

then the sliding mode algorithm (2) can be used to reconstruct the state of system (5) by measurements of the output $y(t)$. Namely, letting $\zeta = [\, \zeta_1 \ \cdots \ \zeta_n \,]^\top$, define the following map

$$\Phi(y,\zeta) = \begin{bmatrix} \zeta_2 - \lambda_{n-1} L^{\frac{1}{n}} |\zeta_1 - y|^{\frac{n-1}{n}} \operatorname{sign}(\zeta_1 - y) \\ \zeta_3 - \lambda_{n-2} L^{\frac{2}{n}} |\zeta_1 - y|^{\frac{n-2}{n}} \operatorname{sign}(\zeta_1 - y) \\ \vdots \\ \zeta_n - \lambda_1 L^{\frac{n-1}{n}} |\zeta_1 - y|^{\frac{1}{n}} \operatorname{sign}(\zeta_1 - y) \\ -\lambda_0 L \operatorname{sign}(\zeta_1 - y) \end{bmatrix}, \tag{7}$$

where $\lambda_0, \lambda_1, \dots, \lambda_{n-1} \in \mathbb{R}_{>0}$ are properly chosen constants[21,27] (see[21] Remark 6.1) and $L \in \mathbb{R}_{>0}$ is a tuning constant. By classical results about sliding mode differentiation[28,11], if the signal $\frac{\mathrm{d}^n y(t)}{\mathrm{d}t^n}$ is L-Lipschitz as a function of t, then the state $\hat{z}(t)$ of the sliding mode differentiator

$$\dot{\hat{z}}(t) = \Phi(y(t), \hat{z}(t)), \tag{8}$$

converges in finite-time to the signal $z(t)$. Thus, under the above assumptions, by Theorem 1, letting

$$K(t,x) = \frac{\partial O(t,x)}{\partial x},$$

one has that the state $\hat{\xi}(t)$ of the observer given by (8) and

$$\dot{\hat{\xi}}(t) = \mu\, K^{-1}(t, \hat{\xi}(t)) \left(\operatorname{sign}(\hat{z}(t) - O(t, \hat{\xi}(t))) - \frac{\partial O(t, \hat{\xi}(t))}{\partial t} \right), \tag{9}$$

locally converges in finite-time[29] to the state of system (5).

The main objective of the remainder of this section is to propose an alternative sliding mode observer that still achieves local, finite-time convergence to the state of system (5) but with simpler dynamics. Toward this objective, the following three assumptions, which adapt Assumptions 1, 2, and 3 to the setting of this section, are made.

Assumption 4. There exist a bounded set $\mathcal{X}$ and $\varepsilon > 0$ such that $x(t) \in \mathcal{X}_\varepsilon$ for all $t \geq 0$.

Assumption 5. The function $x \mapsto O(t,x)$ is $\mathcal{C}^1$ and bijective over $\mathcal{X}$ for all $t \geq 0$, its inverse $z \mapsto O^{-1}(t,z)$ is $\mathcal{C}^1$ for all $t \geq 0$, and there exist constants $\varsigma_1, \varsigma_2 \in \mathbb{R}_{>0}$ such that, for all $x, \hat{x} \in \mathcal{X}$ and all $t \geq 0$,

$$\varsigma_1 \left\| O(t,x) - O(t,\hat{x}) \right\|_2 \leq \left\| x - \hat{x} \right\|_2 \leq \varsigma_2 \left\| O(t,x) - O(t,\hat{x}) \right\|_2. \tag{10}$$

Assumption 6. The signal $\frac{\mathrm{d}^n y(t)}{\mathrm{d}t^n}$ is L-Lipschitz as a function of t,

Under Assumptions 4, 5, and 6, one has that $K(t,x)$ has full rank for all $x \in \mathcal{X}$ and all $t \geq 0$. Hence, consider the system

$$\dot{\hat{x}}(t) = K^{-1}(t,\hat{x}(t)) \left(\Phi(y(t), O(t,\hat{x}(t))) - \frac{\partial O(t,\hat{x}(t))}{\partial t} \right), \tag{11}$$

where the function Φ is defined as in (7). The following theorem states that system (11) is a local, finite-time observer for system (5).

Theorem 3
Let Assumptions 4, 5, and 6 hold, and let $\tilde{x}(t) = x(t) - \hat{x}(t)$. There exists $\delta^\star \in \mathbb{R}_{>0}$ such that if $\|\tilde{x}(0)\|_2 \leq \delta^\star$, then the state $\hat{x}(t)$ of system (11) converges in finite-time to the state $x(t)$ of system (5).

Proof. Let $\hat{z}(t) = O(t,\hat{x}(t))$, and using the convention $\inf_{t\in\emptyset} t = +\infty$, let

$$T := \inf\{t \in \mathbb{R}_{\geq 0} : \tilde{x}(t) \notin \mathcal{B}_\varepsilon\}.$$

Hence, since $\hat{x}(t) = x(t) + \tilde{x}(t)$ and $x(t) \in \mathcal{X}_\varepsilon$, under Assumption 4, one has that $\hat{x}(t) \in \mathcal{X}$ for all $t \in [0,T)$ and there is no finite escape time for all $t \in [0,T)$ even in the case that $T = +\infty$. Thus, for all $t \in [0,T)$, one has that

$$\begin{aligned}\dot{\hat{z}}(t) &= K(t,\hat{x}(t))\dot{\hat{x}}(t) + \frac{\partial O(t,\hat{x}(t))}{\partial t} \\ &= \Phi(y(t),\hat{z}(t)).\end{aligned}$$

By defining $\tilde{z}(t) = z(t) - \hat{z}(t)$, under Assumption 6, if the constants $\lambda_0, \dots, \lambda_{n-1}$ in (7) are suitably chosen[27], then there exists a function $V(\tilde{z})$ satisfying, for all $t \in [0,T)$,

$$\begin{aligned}\beta_1(\|\tilde{z}\|_2) \leq V(\tilde{z}) \leq \beta_2(\|\tilde{z}\|_2), \\ \frac{\mathrm{d}}{\mathrm{d}t} V(\tilde{z}(t)) \leq -\gamma\, V^{\frac{2n-2}{2n-1}}(\tilde{z}(t)),\end{aligned}$$

for some $\gamma \in \mathbb{R}_{\geq 0}$ and some functions $\beta_1, \beta_2 \in \mathcal{K}_\infty$. Under Assumption 5, this implies that, for all $t \in [0,T)$,

$$\begin{aligned}V(\tilde{z}(t)) &\leq \max\left\{ \frac{1}{(2n-1)^{2n-1}} \left((2n-1)\, V(\tilde{z}(0))^{\frac{1}{2n-1}} - \gamma\, t \right)^{2n-1}, 0 \right\} \\ &\leq \max\left\{ \frac{1}{(2n-1)^{2n-1}} \left((2n-1)\, \beta_2^{\frac{1}{2n-1}}(\|\tilde{z}(0)\|_2) - \gamma\, t \right)^{2n-1}, 0 \right\} \\ &\leq \max\left\{ \frac{1}{(2n-1)^{2n-1}} \left((2n-1)\, \beta_2^{\frac{1}{2n-1}} \left(\frac{1}{\varsigma_1} \|\tilde{x}(0)\|_2 \right) - \gamma\, t \right)^{2n-1}, 0 \right\}.\end{aligned}$$

Therefore, by considering that $V(\tilde{z}(t)) \geq \beta_1(\|\tilde{z}(t)\|_2) \geq \beta_1\left(\frac{1}{\varsigma_2}\|\tilde{x}(t)\|_2\right)$, it results that, for all $t \in [0,T)$,

$$\|\tilde{x}(t)\|_2 \leq \max\left\{ \varsigma_2\, \beta_1^{-1}\left(\frac{1}{(2n-1)^{2n-1}} \left((2n-1)\, \beta_2^{\frac{1}{2n-1}} \left(\frac{1}{\varsigma_1} \|\tilde{x}(0)\|_2 \right) - \gamma\, t \right)^{2n-1} \right), 0 \right\}.$$

This implies that there exists $\delta^\star$ such that if $\|\tilde{x}(0)\|_2 \leq \delta^\star$, then $T = +\infty$ and $\tilde{x}$ converges in finite-time to 0. □

In the following remark, the properties of the observers (8), (9) and (11) are compared.

Remark 3. All the observers (8), (9) and (11) are capable of locally estimating in finite-time the state of system (5) under similar assumptions. However, while the dimension of the state of the observer (8), (9) is $2n$, the dimension of the state of the observer (11) is n. Hence, the latter observer is simpler to be implemented. This is due to the fact that the observer (8), (9) disjointly estimates the time-derivatives of the output and of the state of system (5) via the sliding mode differentiator (8) and the sliding mode inversion algorithm (9), whereas such two tasks are carried out jointly by the observer (11). Furthermore, while the dynamical inversion algorithm (9) requires n measurements in order to reconstruct the state of system (5), which are provided by the sliding mode differentiator (8) when it is used as a state observer, the estimator (11) reconstructs the state of system (5) just by using measurements of its output $y(t) \in \mathbb{R}$.

As for system (2), the convergence properties of the observer (11) are global in the case that Assumption 5 hold with $\mathcal{X} = \mathbb{R}^n$, as formally stated in the following corollary.

Corollary 2
Let Assumption 5 hold with $\mathcal{X} = \mathbb{R}^n$ and let Assumption 6 hold. Then the solution $\hat{x}(t)$ of system (11) converges in finite-time to the state $x(t)$ of system (5).

Proof. If Assumption 5 holds with $\mathcal{X} = \mathbb{R}^n$, then $K(t, x)$ has full rank for all $x \in \mathbb{R}^n$ and all $t \geq 0$. Thus, using the same construction employed in the proof of Theorem 3, the estimation error $\tilde{x}(t)$ converges in finite-time to 0. □

The following remark shows how to apply the sliding observer (11) to estimate the state of linear, time-variant systems.

Remark 4. If system (5) is linear, i.e., its dynamics read as

$$\dot{x}(t) = A(t)\, x(t), \tag{12a}$$

$$y(t) = C(t)\, x(t), \tag{12b}$$

with $A(t) \in \mathbb{R}^{n\times n}$ and $C(t) \in \mathbb{R}^{1\times n}$ for all $t \geq 0$, the dynamics of the observer (11) can be given in a more explicit form. In particular, by defining the time-varying observability matrix [30] (see also [31] Sec. 6.8)

$$\Theta(t) = \begin{bmatrix} C_0(t) \\ C_1(t) \\ \vdots \\ C_{n-1}(t) \end{bmatrix},$$

where

$$C_0(t) = C(t),$$
$$C_i(t) = C_{i-1}(t)A(t) + \frac{\partial}{\partial t} C_{i-1}(t), \quad i = 1, \dots, n-1,$$

one has that the dynamics of the observer (11) read as

$$\dot{\hat{x}}(t) = \Theta^{-1}(t) \left(\Phi(y(t), \Theta(t)\, \hat{x}(t))) - \frac{\mathrm{d}\Theta(t)}{\mathrm{d}t}\, \hat{x}(t) \right). \tag{13}$$

By Corollary 2, if $\operatorname{rank}(\Theta(t)) = n$ for all $t \geq 0$, i.e., system (5) is uniformly observable with respect to time t, then the state of the sliding mode observer (13) globally converges in finite-time to the state $x(t)$ of system (12).

This section is concluded by characterizing the properties of the observer (11) in the presence of measurement noise. Namely, consider the following theorem.

Theorem 4
Let Assumptions 4, 5, and 6 hold, suppose that an additive noise $d(t)$ is added to the output $y(t)$, and define $\zeta(t) = [\, d(t) \ \frac{\mathrm{d}d(t)}{\mathrm{d}t} \ \cdots \ \frac{\mathrm{d}^n d(t)}{\mathrm{d}t^n} \,]^\top$. There exists $\delta^\star \in \mathbb{R}_{>0}$ and $Z^\star \in \mathbb{R}_{>0}$ such that if $\|\tilde{x}(0)\|_2 \leq \delta^\star$ and $\|\zeta(t)\|_2 \leq Z^\star$ for all $t \geq 0$, then the estimation error $\tilde{x}(t) = x(t) - \hat{x}(t)$ satisfies, for all $t \geq 0$,

$$\|\tilde{x}(t)\|_2 \leq \vartheta \left(\|\tilde{x}(0)\|_2, t \right) + \varrho \left(\sup_{\tau \geq 0} \|\zeta(\tau)\|_2 \right), \tag{14}$$

for some $\vartheta \in \mathcal{KL}$ and some $\varrho \in \mathcal{K}$.

Proof. Letting $\tilde{x}$, T, and $\tilde{z}$ be defined as in the proof of Theorem 3, one has that [32,33] there exist a function $\theta \in \mathcal{KL}$ and a function $\rho \in \mathcal{K}$ such that, for all $t \in [0, T)$,

$$\begin{aligned} \|\tilde{z}(t)\|_2 &\leq \theta \left(\|\tilde{z}(0)\|_2, t \right) + \rho \left(\sup_{\tau \geq 0} \|\zeta(\tau)\|_2 \right) \\ &\leq \theta \left(\frac{1}{\varsigma_1} \|\tilde{x}(0)\|_2, t \right) + \rho \left(\sup_{\tau \geq 0} \|\zeta(\tau)\|_2 \right). \end{aligned}$$

Therefore, since under Assumption 5 one has that $\|\tilde{z}(t)\|_2 \geq \frac{1}{\varsigma_2} \|\tilde{x}(t)\|_2$, one has that, for all $t \in [0, T)$,

$$\|\tilde{x}(t)\|_2 \leq \varsigma_2\, \theta \left(\frac{1}{\varsigma_1} \|\tilde{x}(0)\|_2, t \right) + \varsigma_2\, \rho \left(\sup_{\tau \geq 0} \|\zeta(\tau)\|_2 \right).$$

Therefore, there exists $\delta^\star \in \mathbb{R}_{>0}$ and $Z^\star \in \mathbb{R}_{>0}$ such that if $\|\tilde{x}(0)\|_2 \leq \delta^\star$ and $\|\zeta(t)\|_2 \leq Z^\star$ for all $t \geq 0$, then $T = +\infty$, thus implying that (14) holds for all $t \geq 0$. □

Remark 5. In order to implement (9), (11), and (13), the dependence of the observability map $O(t, x)$ on t has to be known a prior. However, following the same reasoning used to prove Theorem 4 and considering that the omission of the term $\frac{\partial O(t,x)}{\partial t}$ in these dynamics acts as a disturbance on the dynamics of the error $\tilde{z}$, there exists $\delta^\star \in \mathbb{R}_{>0}$ and $O^\star \in \mathbb{R}_{>0}$ such that if $\|\tilde{x}(0)\|_2 \leq \delta^\star$ and $\|\frac{\partial O(t,x)}{\partial t}\|_2 \leq O^\star$ for all $t \geq 0$ and all $x \in \mathcal{X}_\epsilon$, then the estimation error $\tilde{x}(t) = x(t) - \hat{x}(t)$ satisfies, for all $t \geq 0$,

$$\|\tilde{x}(t)\|_2 \leq \vartheta\left(\|\tilde{x}(0)\|_2, t\right) + \rho,$$

for some $\vartheta \in \mathcal{KL}$ and some $\rho > 0$.

Remark 6. By[32] Theorem 4, results wholly similar to the ones given in Theorem 4 can be stated in the case of discrete sampling. In particular, by[34], if the sliding mode differentiator (8) is implemented with discrete samples with sampling time τ, then, in the absence of measurement noise, there exist constants $\theta_0, \dots, \theta_{n-1}$ such that $|y(t) - \hat{z}_1(t)| \leq \theta_0 \tau^n$, $|\dot{y}(t) - \hat{z}_2(t)| \leq \theta_1 \tau^{n-1}, \dots, |\frac{\mathrm{d}^{n-1} y(t)}{\mathrm{d}t^{n-1}} - \hat{z}_n| \leq \theta_{n-1}\tau$, for all sufficiently large times t.

4 | SPACE APPLICATIONS

The main objective of this section is to demonstrate the practical usefulness of the design techniques proposed in Sections 2 and 3 to solve relevant space problems. In particular, in Section 4.1, it is shown how the observer (11) can be used to estimate unmeasured angular velocities of an axial symmetric spacecraft. In Section 4.2, it is shown how the sliding mode inversion algorithm (2) can be used to estimate the inertia parameters of a spacecraft. Finally, in Section 4.3, the observer (11) is used to estimate a Keplerian orbital element given measurements of the other five ones.

4.1 | Estimation of unmeasured angular velocity

An important operation in several aerospace missions is estimation of the spacecraft (or plane) angular velocity. Indeed, this variable is often used for attitude control and other relevant tasks. Clearly, the angular velocity of a body can be measured by means of a gyroscope but the availability of an effective angular velocity estimator is in any case advantageous for several reasons: accuracy improvement, cost reduction, redundancy, fault tolerance and simpler system design.

The rotation dynamics of a satellite can be described by writing Euler's equations in a set of principal axes (see[35] Equation (4.5.1'))

$$I_1 \dot{\omega}_1(t) + (I_3 - I_2)\,\omega_2(t)\,\omega_3(t) = M_1, \tag{15a}$$
$$I_2 \dot{\omega}_2(t) + (I_1 - I_3)\,\omega_3(t)\,\omega_1(t) = M_2, \tag{15b}$$
$$I_3 \dot{\omega}_3(t) + (I_2 - I_1)\,\omega_1(t)\,\omega_2(t) = M_3. \tag{15c}$$

Assuming that the satellite is axial symmetric, that no transversal torques are applied, and that one of the two transverse and the spin angular velocities are measured, such dynamics can be rewritten as

$$\dot{\omega}_1(t) = -\Omega(t)\,\omega_2(t), \tag{16a}$$
$$\dot{\omega}_2(t) = \Omega(t)\,\omega_1(t), \tag{16b}$$
$$y(t) = \omega_1(t), \tag{16c}$$

where $\Omega(t)$ is the spin velocity and $\omega_1(t), \omega_2(t)$ are the two transverse velocities. The main objective of this section is to estimate the angular velocity ω_2 from measurements of ω_1 and $\Omega(t)$.

In this tutorial example, if $\Omega(t) \neq 0$ for all $t \geq 0$, then an estimate $\hat{\omega}_2$ of the state ω_2 of system (16) can be obtained by estimating the time derivative $y_1(t) = \dot{y}(t)$ of the measured output $y(t)$, e.g., by using the sliding mode differentiator

$$\dot{\hat{y}}_0(t) = \hat{y}_1 - \lambda_1 L^{\frac{1}{2}} |\hat{y}_0 - y|^{\frac{1}{2}} \operatorname{sign}(\hat{y}_0 - y), \tag{17a}$$
$$\dot{\hat{y}}_1(t) = -\lambda_0 L \operatorname{sign}(\hat{y}_0 - y), \tag{17b}$$

and letting

$$\hat{\omega}_2(t) = -\frac{1}{\Omega(t)}\hat{y}_1(t). \tag{17c}$$

On the other hand, the observer (11) for system (16) reads as

$$\dot{\hat{\omega}}_1(t) = -\Omega(t)\,\hat{\omega}_2(t) - \lambda_1\, L^{\frac{1}{2}}\,|\hat{\omega}_1(t) - y(t)|^{\frac{1}{2}}\,\mathrm{sign}(\hat{\omega}_1(t) - y(t)), \tag{18a}$$

$$\dot{\hat{\omega}}_2(t) = -\frac{1}{\Omega(t)}\left(-\lambda_0\, L\,\mathrm{sign}(\hat{\omega}_1(t) - y(t)) - \hat{\omega}_2(t)\,\dot{\Omega}(t)\right). \tag{18b}$$

It is worth pointing out that the observer (18) exactly implements the observer (17) in the original coordinates. In fact, it can be easily observed that system (17) is diffeomorphic to system (18) via the diffeomorphism

$$\begin{bmatrix} \hat{\omega}_1 \\ \hat{\omega}_2 \end{bmatrix} = \begin{bmatrix} \hat{y}_0 \\ -\frac{1}{\Omega(t)}\hat{y}_1 \end{bmatrix},$$

that is well defined if $\Omega(t) \neq 0$ for all $t \geq 0$.

A numerical simulation has been carried out to test the effectiveness of the observer (18) letting $\lambda_0 = 1.1$, $\lambda_1 = 1.5$, $L = 20$, $\Omega = 2 + \sin(t)$, $\omega_1(0) = 1$, $\omega_2(0) = -1$, $\hat{\omega}_1(0) = 0$, and $\hat{\omega}_2(0) = 0$. The results of such a numerical simulation are shown in Figure 1.

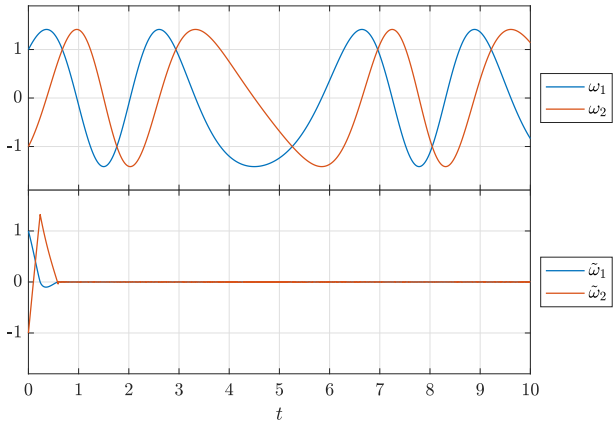

FIGURE 1 Results of the numerical simulation for the observer (18) in absence of measurement noise.

As shown by Figure 1 the observer (18) is capable of reconstructing the state of system (16) in finite-time if measurement noise is absent.

Another simulation has been carried out to test the effectiveness of the observer (18) in the presence of a small band-limited white noise (power 10^{-12} and sampling time 10^{-4}). Figure 2 depicts the results of this simulation. As shown by Figure 2, the

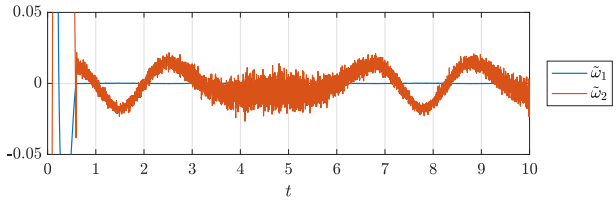

FIGURE 2 Results of the numerical simulation for the observer (18) in the presence of measurement noise.

observer (18) presents good performance even in the presence of measurement noise.

Finally, in order to compare the proposed sliding mode observer with other techniques taken from the literature, another numerical simulation has been carried out using the Kalman-Bucy filter[36,37,38]

$$\dot{\hat{\omega}}(t) = \begin{bmatrix} 0 & -\Omega(t) \\ \Omega(t) & 0 \end{bmatrix} \hat{\omega}(t) + P(t) \begin{bmatrix} y(t) - \hat{\omega}_1(t) \\ 0 \end{bmatrix}, \tag{19a}$$

$$\dot{P}(t) = \begin{bmatrix} \alpha & -\Omega(t) \\ \Omega(t) & \alpha \end{bmatrix} P(t) + P(t) \begin{bmatrix} \alpha & \Omega(t) \\ -\Omega(t) & \alpha \end{bmatrix} + I - P(t) \begin{bmatrix} 1 & 0 \\ 0 & 0 \end{bmatrix} P(t), \tag{19b}$$

with $\alpha = 10$, initialized at $\hat{\omega}(0) = [\,0 \;\; 0\,]^\top$ and $P(0) = I$, where I denotes the identity matrix, to estimate the state of system (16). The results of such a simulation (without measurement noise) are shown in Figure 3.

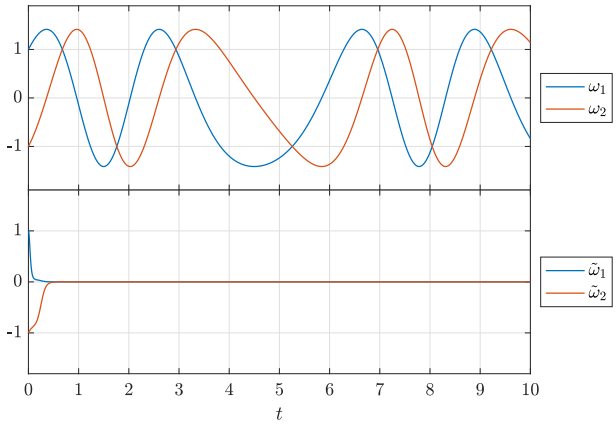

FIGURE 3 Results of the numerical simulation for the Kalman-Bucy filter.

As shown by Figure 3, also the Kalman-Bucy filter is capable of estimating the state of system (16). However, while the state of the observer (18) converges in finite-time to the state of system (16), the convergence of the Kalman-Bucy filter (19) is exponential. Namely, in the absence of measurement noise, one has that there exists a finite time such that the state of the observer (18) is exactly equal to the one of system (15), whereas the state of the Kalman-Bucy filter converges exponentially to the state of system (15). Finally, for fairness of comparison, a numerical simulation has been carried out to evaluate the sentivity of the Kalman-Bucy filter to measurement noise by adding to the output a small band-limited white noise (power 10^{-12} and sampling time 10^{-4}). The results of such a simulation are shown in Figure 4.

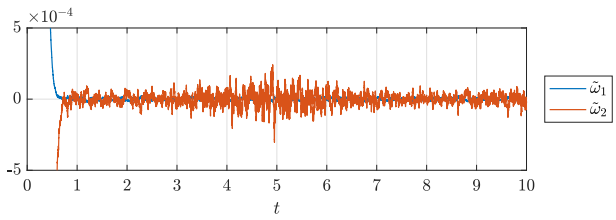

FIGURE 4 Results of the numerical simulation for the Kalman-Bucy filter in the presence of measurement noise.

As shown by Figure 4, the Kalman-Bucy filter (19) has improved filtering properties with respect to the observer (18) in the presence of small band-limited white measurement noise. This is essentially due to the fact that the proposed observer is based on the time derivatives of the measured output and hence, if such a signal is affected by high-frequency disturbances, then the gathered estimates are affected by large estimation errors.

4.2 | Inertia matrix estimation

Space debris orbiting around the Earth are becoming a major problem that could impair the future of space missions. Among the different approaches to this problem proposed in recent years, a possible one consists in an autonomous spacecraft that performs a rendezvous and docking maneuver, collects a debris and then moves it to a parking orbit. When the spacecraft collects a debris, several parameters like the mass and inertia matrix may change substantially, seriously affecting the spacecraft control performance. The availability of an algorithm able to estimate such parameters when the debris is captured is thus of paramount importance.

The main objective of this section is to show how the sliding mode inversion technique proposed in Section 2 can be used to estimate the inertia matrix in (15) from measurements of the angular velocities ω_1, ω_2, and ω_3.

Toward this objective, note that sliding mode differentiators of the form[28]

$$\dot{\hat{\omega}}_i(t) = \hat{\alpha}_i(t) - \lambda_1 L^{\frac{1}{2}} |\hat{\omega}_i(t) - \omega_i(t)|^{\frac{1}{2}} \operatorname{sign}(\hat{\omega}_i(t) - \omega_i), \tag{20a}$$

$$\dot{\hat{\alpha}}_i(t) = -\lambda_0 L \operatorname{sign}(\hat{\omega}_i(t) - \omega_i(t)). \tag{20b}$$

where $\hat{\alpha}_i$ is an estimate of $\dot{\omega}_i$, $i = 1, \dots, 3$, can be used to estimate the time derivatives of the angular velocities ω_1, ω_2, and ω_3 from their measurements in finite-time. Thus, by defining the map

$$h(t, I) = \begin{bmatrix} \frac{I_2 - I_3}{I_1} \omega_2(t)\, \omega_3(t) + \frac{M_1(t)}{I_1} \\ \frac{I_3 - I_1}{I_2} \omega_3(t)\, \omega_1(t) + \frac{M_2(t)}{I_2} \\ \frac{I_1 - I_2}{I_3} \omega_1(t)\, \omega_2(t) + \frac{M_3(t)}{I_3} \end{bmatrix},$$

and noticing that

$$\dot{\omega}(t) = h(t, I),$$

the technique given in Section 2 together with the sliding differentiator given in (20) can be used to estimate the parameters I_1, I_2, and I_3 from measurements of ω_1, ω_2, and ω_3. Namely, letting $J(t, I) = \frac{\partial h(t, I)}{\partial I}$,

$$J(t, I) = \begin{bmatrix} -\frac{M_1(t)}{I_1^2} - \frac{(I_2 - I_3)\omega_2(t)\omega_3(t)}{I_1^2} & \frac{\omega_2(t)\omega_3(t)}{I_1} & -\frac{\omega_2(t)\omega_3(t)}{I_1} \\ -\frac{\omega_1(t)\omega_3(t)}{I_2} & -\frac{M_2(t)}{I_2^2} - \frac{(I_3 - I_1)\omega_1(t)\omega_3(t)}{I_2^2} & \frac{\omega_1(t)\omega_3(t)}{I_2} \\ \frac{\omega_1(t)\omega_2(t)}{I_3} & -\frac{\omega_1(t)\omega_2(t)}{I_3} & -\frac{M_3(t)}{I_3^2} - \frac{(I_1 - I_2)\omega_1(t)\omega_2(t)}{I_3^2} \end{bmatrix},$$

the parameter vector $I = [\, I_1 \;\; I_2 \;\; I_3 \,]^\top$ can be estimated as

$$\dot{\hat{I}}(t) = \mu\, J^{-1}(t, \hat{I}) \operatorname{sign}(\hat{\alpha}(t) - h(t, \hat{I})), \tag{21}$$

where $\hat{\alpha} = [\, \hat{\alpha}_1 \;\; \hat{\alpha}_2 \;\; \hat{\alpha}_3 \,]^\top$ is the estimate of $\dot{\omega}$ obtained via (20).

A numerical simulation has been carried out to test the estimation algorithm (20), (21) letting $\lambda_0 = 1.1$, $\lambda_1 = 1.5$, $L = 100$, $\mu = 10$, $\hat{\omega}_i(0) = 0$, $\hat{\alpha}_i(0) = 0$, $i = 1, 2, 3$, and initializing $\hat{I}(0)$ at random. The results of such a simulation are shown in Figure 5.

As shown by Figure 5, thanks to the use of the sliding differentiator (20) and of the sliding inversion algorithm (4), the state of system (20), (21) converges in finite time to the values of the inertia parameters I_1, I_2, and I_3.

4.3 | Estimation of unmeasured orbital elements

Consider a spacecraft traveling in a orbit around a planet. The Keplerian orbital elements (OEs) are six quantities that univocally define the geometric characteristics of the orbit and the position of the spacecraft in the orbit. Clearly, determination of the OEs is fundamental in many space missions but, in certain situations, only some of the OEs are measured and the others have to be estimated from the available measurements.

The OEs of an orbit are the following: x_1 is the semi-major axis, x_2 is the eccentricity, x_3 is the inclination, x_4 is the right ascension of the ascending node, x_5 argument of the periapsis, x_6 is the true anomaly (see[39] Section 5.3 for their formal definition). The spacecraft traveling on the orbit is subject to external forces, which typically include the thruster force and different types of perturbations. Such forces produce an acceleration u_1 in the direction of the radius vector, positive in the direction of increasing radial distance, an acceleration u_2 perpendicular to the radius vector in the orbital plane, positive in the direction of increasing longitude, and an acceleration u_3 perpendicular to the orbital plane, positive towards the north pole.

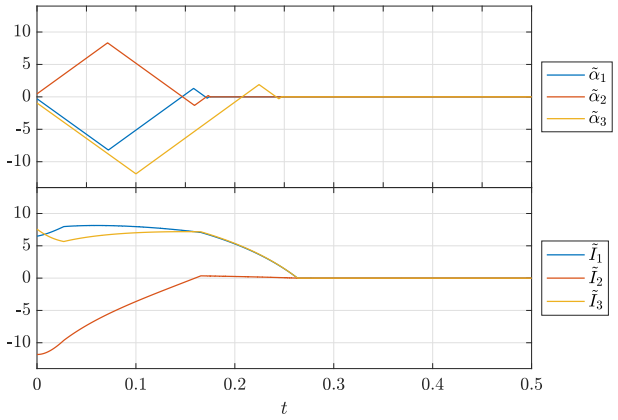

FIGURE 5 Results of the numerical simulation for the estimation algorithm (20), (21). The symbols $\tilde{\alpha}_i$ and $\tilde{I}_i$ denote the estimation errors $\alpha_i - \hat{\alpha}_i$ and $I_i - \hat{I}_i$, respectively.

The dynamics of the OEs is described by a set of six first-order differential equations called Gauss planetary equations, which can be written as follows (see[39] Section 5.3.1):

$$\dot{x}_1 = \frac{2\left(u_1 x_2 \sin\left(x_6\right) + u_2 x_2 \cos\left(x_6\right) + u_2\right)}{\sqrt{1-x_2^2}\sqrt{\frac{\eta}{x_1^3}}}, \tag{22a}$$

$$\dot{x}_2 = \frac{\sqrt{1-x_2^2}\left(u_2\left(x_2 + \cos\left(x_6\right)\left(x_2\cos\left(x_6\right)+2\right)\right) + u_1 \sin\left(x_6\right)\left(x_2\cos\left(x_6\right)+1\right)\right)}{\sqrt{\frac{\eta}{x_1^3}}\left(x_1 + x_2 x_1 \cos\left(x_6\right)\right)}, \tag{22b}$$

$$\dot{x}_3 = \frac{u_2\left(\sqrt{1-x_2^2}+1\right)\sin\left(x_6\right) - \cos\left(x_6\right)\left(u_1 x_2 \cos\left(x_6\right) + u_1 - u_2 x_2 \sin\left(x_6\right)\right) - u_3 x_2 \sin\left(x_3+x_6\right)\cot\left(x_5\right)}{x_1 \frac{x_2}{\sqrt{1-x_2^2}}\sqrt{\frac{\eta}{x_1^3}}\left(x_2\cos\left(x_6\right)+1\right)}, \tag{22c}$$

$$\dot{x}_4 = \frac{u_3\sqrt{1-x_2^2}\sin\left(x_3+x_6\right)\csc\left(x_5\right)}{\sqrt{\frac{\eta}{x_1^3}}\left(x_1 + x_2 x_1 \cos\left(x_6\right)\right)}, \tag{22d}$$

$$\dot{x}_5 = \frac{u_3\sqrt{1-x_2^2}\cos\left(x_3+x_6\right)}{\sqrt{\frac{\eta}{x_1^3}}\left(x_1 + x_2 x_1 \cos\left(x_6\right)\right)}, \tag{22e}$$

$$\dot{x}_6 = \frac{\sqrt{1-x_2^2}\left(u_1\cos\left(x_6\right)\left(x_2\cos\left(x_6\right)+1\right) - u_2\sin\left(x_6\right)\left(x_2\cos\left(x_6\right)+2\right)\right)}{x_1 x_2\sqrt{\frac{\eta}{x_1^3}}\left(x_2\cos\left(x_6\right)+1\right)}, \tag{22f}$$

and η is a constant called the gravitational parameter.

Assuming that just the variables x_1, x_2, x_3, and x_4 can be measured, the technique outlined in Section 3 has been used to design an observer for the true anomaly x_6 using the dynamics (22e). Namely, consider the time-varying system

$$\dot{x}_5 = \frac{u_3\sqrt{1-x_2^2}\cos\left(x_3+x_6\right)}{\sqrt{\frac{\eta}{x_1^3}}\left(x_1+x_2x_1\cos\left(x_6\right)\right)}, \tag{23a}$$

$$\dot{x}_6 = \frac{\sqrt{1-x_2^2}\left(u_1\cos\left(x_6\right)\left(x_2\cos\left(x_6\right)+1\right)-u_2\sin\left(x_6\right)\left(x_2\cos\left(x_6\right)+2\right)\right)}{x_1x_2\sqrt{\frac{\eta}{x_1^3}}\left(x_2\cos\left(x_6\right)+1\right)}, \tag{23b}$$

$$y = x_5, \tag{23c}$$

where the signals $x_1(t)$, $x_2(t)$, $x_3(t)$, and $x_4(t)$ are assumed to be provided by (22) and measurable.

The observability map of system (23) is

$$O(t,x_5,x_6) = \begin{bmatrix} x_5 \\ \frac{u_3(t)\sqrt{1-x_2^2(t)}\cos\left(x_3(t)+x_6\right)}{x_1(t)\sqrt{\frac{\eta}{x_1^3(t)}}\left(x_2(t)\cos\left(x_6\right)+1\right)} \end{bmatrix}.$$

Therefore, one has that

$$J(t,x_5,x_6) = \begin{bmatrix} 1 & 0 \\ 0 & -\frac{u_3(t)\sqrt{1-x_2^2(t)}\left(\sin\left(x_3(t)+x_6\right)+x_2(t)\sin\left(x_3(t)\right)\right)}{x_1(t)\sqrt{\frac{\eta}{x_1(t)^3}}\left(x_2(t)\cos\left(x_6\right)+1\right)^2} \end{bmatrix},$$

$$\frac{\partial O(t,x_5,x_6)}{\partial t} = \begin{bmatrix} 0 & 0 & 0 & 0 \\ \frac{u_3(t)\sqrt{1-x_2^2(t)}\cos\left(x_3(t)+x_6\right)}{2x_1^2(t)\sqrt{\frac{\eta}{x_1^3(t)}}\left(x_2(t)\cos\left(x_6\right)+1\right)} & -\frac{u_3(t)\cos\left(x_3(t)+x_6\right)\left(x_2(t)+\cos\left(x_6\right)\right)}{x_1(t)\sqrt{1-x_2^2(t)}\sqrt{\frac{\eta}{x_1^3(t)}}\left(x_2(t)\cos\left(x_6\right)+1\right)^2} & \frac{\sqrt{1-x_2(t)^2}\cos\left(x_3(t)+x_6\right)}{x_1(t)\sqrt{\frac{\eta}{x_1^3(t)}}\left(x_2(t)\cos\left(x_6\right)+1\right)} & -\frac{u_3(t)\sqrt{1-x_2^2(t)}\sin\left(x_3(t)+x_6\right)}{x_1(t)\sqrt{\frac{\eta}{x_1^3(t)}}\left(x_2(t)\cos\left(x_6\right)+1\right)} \end{bmatrix} \begin{bmatrix} \dot{x}_1(t) \\ \dot{x}_2(t) \\ \dot{u}_3(t) \\ \dot{x}_3(t) \end{bmatrix}.$$

A numerical simulation has been carried out to test the effectiveness of the observer (11) with the two functions above, where the values of $\dot{x}_1$, $\dot{x}_2$, $\dot{u}_3$, and $\dot{x}_3$ have been estimated by using sliding mode differentiators wholly similar to (20). In such a simulation, the initial conditions have been set to $x_1(0) = 6723\,\text{km}$, $x_2(0) = 0.15$, $x_3(0) = 3.04\,\text{rad}$, $x_4(0) = 3.28\,\text{rad}$, $x_5(0) = 0.9\,\text{rad}$, $x_6(0) = 2.44\,\text{rad}$, the value η has been set to $3.986 \cdot 10^5\,\text{km}^3/\text{s}^2$ (which corresponds to the Earth gravitational parameter), the control inputs have been set to $u_1 = 0$, $u_2 = 1$, and $u_3 = 10$, whereas the parameters of the sliding mode differentiator have been set to $\lambda_0 = 1.1$, $\lambda_1 = 1.5$, and $L = 100$. Figure 6 depicts the results of such a simulation.

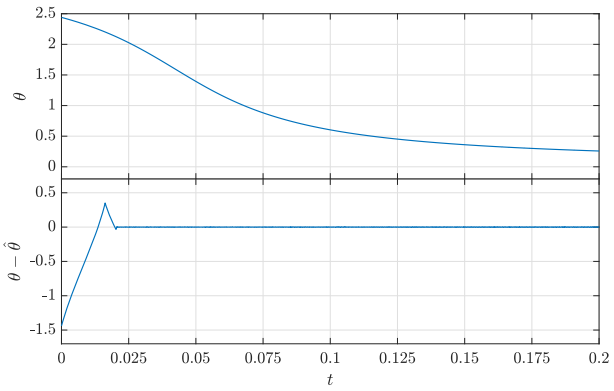

FIGURE 6 Results of the numerical simulation for the estimator of the true anomaly.

As shown by Figure 6, the proposed sliding mode observer is capable of reconstructing the true anomaly in finite-time.

5 | CONCLUSIONS

In this paper, sliding mode techniques have been proposed either to invert a time-varying map or to estimate the state of a time-varying nonlinear system. In particular, the inversion algorithm has been designed by exploiting a modified version of the Newton algorithm that ensures local, finite-time convergence of the estimation error to zero. On the other hand, the proposed state observer has been designed by using the inverse of the Jacobian of the observability map of the system to implement a sliding mode differentiator in the original coordinates. Finally, it has been shown how these two techniques can be used to solve relevant space problems, such as the estimation of the angular velocity of an axial symmetric satellite, the estimation of the inertia parameters of an orbiting object from measurements of its angular velocities, and the estimation of a Keplerian orbital element given measurements of the other five ones.

References

1. Besançon G. *Nonlinear observers and applications*. Springer . 2007.
2. Luenberger DG. *Introduction to dynamic systems; theory, models, and applications*. John Wiley and Sons . 1979.
3. Kalman RE. A new approach to linear filtering and prediction problems. *J. Basic Eng.* 1960; 82(1): 35–45.
4. Bonnabel S, Slotine JJ. A contraction theory-based analysis of the stability of the deterministic extended Kalman filter. *IEEE Trans. Autom. Control* 2015; 60(2): 565–569.
5. Gordon NJ, Salmond DJ, Smith AF. Novel approach to nonlinear/non-Gaussian Bayesian state estimation. In: . 140. IET. ; 1993: 107–113.
6. Kazantzis N, Kravaris C. Nonlinear observer design using Lyapunov's auxiliary theorem. *Syst. Control Lett.* 1998; 34(5): 241–247.
7. Ciccarella G, Dalla Mora M, Germani A. A Luenberger-like observer for nonlinear systems. *Int. J. Control* 1993; 57(3): 537–556.
8. Krener AJ, Isidori A. Linearization by output injection and nonlinear observers. *Syst. Control Lett.* 1983; 3(1): 47–52.
9. Astolfi D, Possieri C. Design of local observers for autonomous nonlinear systems not in observability canonical form. *Automatica* 2019; 103: 443–449.
10. Gauthier JP, Kupka I. *Deterministic observation theory and applications*. Cambridge Univ. Pr. . 2001.
11. Levant A. Higher-order sliding modes, differentiation and output-feedback control. *Int. J. Control* 2003; 76(9-10): 924–941.
12. Tornambe A. High-gain observers for non-linear systems. *Int. J. Syst. Sci.* 1992; 23(9): 1475–1489.
13. Moreno JA, Osorio M. Strict Lyapunov functions for the super-twisting algorithm. *IEEE Trans. Autom. Control* 2012; 57(4): 1035–1040.
14. Nicosia S, Tornambe A, Valigi P. A solution to the generalized problem of nonlinear map inversion. *Syst. Control Lett.* 1991; 17(5): 383–394.
15. Nicosia S, Tornambe A, Valigi P. Nonlinear map inversion via state observers. *Circuits Syst. Signal Proces.* 1994; 13(5): 571–589.
16. Menini L, Possieri C, Tornambe A. Newton-like algorithms for the inversion of switched maps. *Automatica* 2019; 104: 228–232.
17. Menini L, Possieri C, Tornambe A. A "practical" observer for nonlinear systems. In: IEEE. ; 2017: 3015–3020.
18. Menini L, Possieri C, Tornambe A. A Newton-like algorithm to compute the inverse of a nonlinear map that converges in finite time. *Automatica* 2018; 89: 411–414.

19. Bernard P, Andrieu V, Praly L. Expressing an observer in preferred coordinates by transforming an injective immersion into a surjective diffeomorphism. *SIAM J. Control Optim.* 2018; 56(3): 2327–2352.

20. Astolfi D, Marconi L, Praly L, Teel AR. Low-power peaking-free high-gain observers. *Automatica* 2018; 98: 169–179.

21. Shtessel Y, Edwards C, Fridman L, Levant A. *Sliding mode control and observation*. Springer . 2014.

22. Andrieu V, Praly L, Astolfi A. Homogeneity in the bi-limit as a tool for observer and feedback design. In: IEEE. ; 2009: 1050–1055.

23. Perruquetti W, Floquet T, Moulay E. Finite-time observers: application to secure communication. *IEEE Trans. Autom. Control* 2008; 53(1): 356–360.

24. Isidori A. *Nonlinear control systems*. Springer . 2013.

25. Filippov AF. *Differential equations with discontinuous right-hand side*. Amer. Math. Soc . 1988.

26. Bhat SP, Bernstein DS. Finite-time stability of continuous autonomous systems. *SIAM J. Control Optim.* 2000; 38(3): 751–766.

27. Cruz-Zavala E, Moreno JA. Levant's Arbitrary-Order Exact Differentiator: A Lyapunov Approach. *IEEE Trans. Autom. Control* 2019; 64(7): 3034-3039.

28. Levant A. Robust exact differentiation via sliding mode technique. *Automatica* 1998; 34(3): 379–384.

29. Possieri C, Vidano S, Novara C. A finite-time local observer in the original coordinates for nonlinear control systems. *IEEE Trans. Autom. Control* 2020; 65(11): 4808-4815.

30. Silverman L, Meadows H. Equivalent realizations of linear systems. *SIAM J. Appl. Math.* 1969; 17(2): 393–408.

31. Chen CT. *Linear Systems Theory and Design*. Oxford University Press . 1999.

32. Levant A. Homogeneity approach to high-order sliding mode design. *Automatica* 2005; 41(5): 823–830.

33. Bernuau E, Efimov D, Perruquetti W, Polyakov A. On homogeneity and its application in sliding mode control. *J. Franklin Inst.* 2014; 351(4): 1866–1901.

34. Levant A. Sliding order and sliding accuracy in sliding mode control. *Int. J. Control* 1993; 58(6): 1247–1263.

35. Sidi MJ. *Spacecraft dynamics and control: a practical engineering approach*. Cambridge Univ. Press . 1997.

36. Bucy RS, Joseph PD. *Filtering for stochastic processes with applications to guidance*. 326. American Mathematical Soc. . 2005.

37. Jazwinski AH. *Stochastic processes and filtering theory*. Courier Corporation . 2007.

38. Reif K, Sonnemann F, Unbehauen R. An EKF-based nonlinear observer with a prescribed degree of stability. *Automatica* 1998; 34(9): 1119–1123.

39. Canuto E, Novara C, Perez Montenegro C, Carlucci D. *Spacecraft Dynamics and Control - the Embedded Model Control Approach*. Butterworth-Heinemann (Elsevier) . 2018.

How to cite this article: Possieri C and Novara C, (2022), Local sliding mode inversion algorithms and state observers with space applications, *Int. J. Robust Nonlinear Control*, .